Critical current and self-consistent order parameter of a superconductor–normal-metal–superconductor junction

Richard A. Riedel, Li-Fu Chang, and Philip F. Bagwell
School of Electrical Engineering, Purdue University, West Lafayette, Indiana 47907
(Received 16 August 1995; revised manuscript received 25 July 1996)

We solve the Bogoliubov–de Gennes (BdG) equations self-consistently for a superconductor–normal-metal–superconductor (SNS) junction embedded in a superconducting wire of uniform width, rather than in a superconducting point contact. Because we avoid geometrically diluting the electrical current density, a significant superfluid flow develops in the uniform width SNS junction, greatly changing the solution of the BdG equations from the SNS point contact. The self-consistent pair-correlation function has a constant phase gradient in the uniform-width SNS junction, forcing spatially extended states to carry the electrical current. Although the bound Andreev levels carry no net current for this type of SNS junction, we find the zero-temperature critical current is still given by $I_c = ev_F/(L+2\xi_0)$. Suppression of the order parameter near the normal-metal interface is also more pronounced in uniform-width SNS junctions, increasing the effective electrical length of the junction to $L^* \geqslant L$ and reducing the critical current. [S0163-1829(96)02246-1]

I. INTRODUCTION

The prediction by Beenakker and van Houten[1] that the critical current of a superconducting quantum point contact should be ''discretized'' in units of $e\Delta/\hbar$ has stimulated much recent work on mesoscopic superconductor–normal-metal–superconductor (SNS) junctions, mesoscopic superconductivity, and the discretization of critical current.[2–14] These calculations mostly ignore the self-consistency condition for the superconducting order parameter, and therefore strictly violate electrical current conservation.[14–18] Some notable recent exceptions include the self-consistent calculation of the electrical current in a superconducting weak link[11] and other structures.[12,13] Reference 11 numerically confirms the argument of Ref. 1 that the self-consistency condition will not affect the final discretized value of the critical current in a superconducting quantum-point contact.

Instead of the constriction geometry of Ref. 11, we investigate the effect of a self-consistent superconducting order parameter for a normal region embedded in a superconducting wire. For the superconducting wire geometry shown in Fig. 1, the widths of the normal-metal region and superconductor are equal. Only several coherence lengths away from each normal-metal–superconductor (NS) junction does the wire widen into the two large superconducting reservoirs. This allows us to neglect superfluid flow perpendicular to the wire, which is important for the superconducting point contact. By restricting our attention to electron transport only in the lowest subband of the superconducting wire, we can therefore use a one-dimensional model for the transport. Current flow in a similar geometry has previously been calculated by Bardeen and Johnson,[19] and further discussed in Ref. 8. Including the self-consistency condition for the superconducting order parameter in a uniform-width SNS junction, as indicated in Sec. II and Appendix A, modifies both the form of the order parameter and the nature of the current-carrying states from those in an SNS point contact.

Since we avoid geometrically diluting the electrical current density at the NS interface, the self-consistency condition for the order parameter strongly influences our calculation. In the non-self-consistent solution of an SNS junction embedded in a point contact, it is usually assumed that a fixed-phase difference in the order parameter is maintained across the SNS junction. The electrical current is then carried by a set of Andreev bound levels localized in the normal region.[1–11] By introducing the self-consistency requirement on the pairing potential $\Delta(x)$, we ensure that the Andreev reflections at each NS interface produce a corresponding superfluid flow in the superconductors. This superfluid flow is small in an SNS point contact, since the superconducting reservoirs are wide compared to the SNS junction. But since we embed the SNS junction in a superconducting wire of equal width, the superfluid flow will produce a relatively

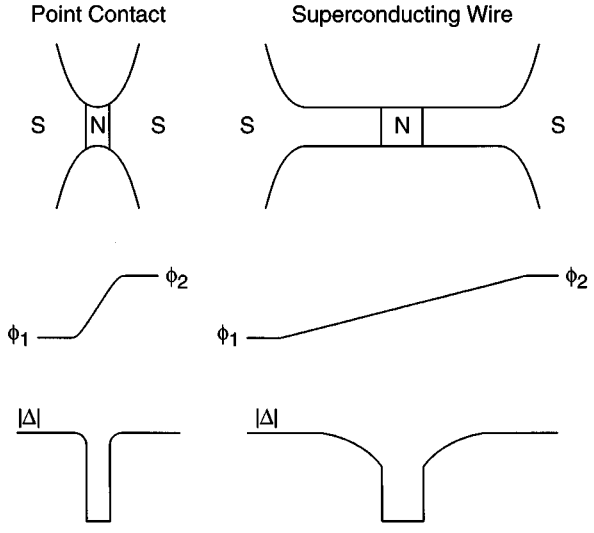

FIG. 1. Geometry of an SNS junction embedded in a superconducting point contact and a superconducting wire. The expected variation of the pairing-correlation function magnitude and phase vs distance in each of the two geometries is also shown.

large phase gradient in the order parameter $\Delta(x)$.

We find in Sec. III that, for a ballistic SNS junction embedded in a superconducting wire, the phase gradient of the pairing-correlation function (order parameter) is constant throughout the entire SNS junction (even inside the normal region), as shown in Fig. 1. The only phase difference that develops across the normal region of the SNS junction arises from this nonzero superfluid flow velocity. The order-parameter phase gradient is approximately constant only for a very limited class of SNS junctions. If any tunnel barrier or impurity is introduced, or if any lateral variation in the junction width is present (within several coherence lengths of the normal region), the order-parameter phase gradient will not be a constant throughout the SNS junction. Although we show the order-parameter phase gradient is very nearly constant only for the one-dimensional SNS junction considered here, we believe it is also nearly a constant in three-dimensional planar, ballistic SNS junctions. This is because a three-dimensional planar, ballistic SNS junction can be viewed as the addition of many one-dimensional SNS junctions in parallel.

For a ballistic SNS junction of uniform width, where the phase gradient is a constant, and when the SNS junction is held at zero temperature, we find that the Andreev bound levels carry zero net electrical current. As shown analytically in Appendix B, all the current flows through the spatially extended ''continuum'' of energy levels located outside the superconducting gap at zero temperature. A uniform-width SNS junction is similar in this respect to a superconducting wire, where all the electrical current is carried outside the superconducting gap. Interrupting the superconducting wire with a normal region, therefore, does not significantly change the energy distribution of the current between the bound and continuum states. This is in contrast to the well-known results for point-contact SNS junctions, where localized Andreev levels do carry a net supercurrent. Indeed, for point-contact SNS junctions having $L \ll \xi_0$, all the supercurrent is carried through the Andreev levels. Despite these differences in the energy distribution of the current, we find in Sec. IV the critical current is $I_c = ev_F/(L+2\xi_0)$ for both junction types at zero temperature.

Placing the SNS junction inside a wire, rather than a point contact, also rounds the magnitude of the order parameter $|\Delta|$ as indicated in Fig. 1. As found by Plehn, Gunsenheimer, and Kümmel,[20] the normal region then has a longer effective electrical length $L^* \geqslant L$, where L is the geometrical length of the normal region. The critical current of the uniform-width SNS junction is then reduced below its value for an SNS point contact, namely, $I_c = ev_F/(L^*+2\xi_0)$. This rounding of the order parameter near each NS boundary in the uniform-width SNS junction results from having only a relatively small number of states near the NS boundary, rather than the larger number of states available to support the order parameter at an NS boundary near the wide superconducting reservoir present in an SNS point contact.

When a strong tunnel barrier or impurity is placed in the SNS junction, forming a superconductor-insulator-superconductor (SIS) junction, a discontinuity in the self-consistent order-parameter phase develops across the impurity. This phase drop is analogous to the voltage drop associated with local electric fields (residual resistivity dipoles) which build up around a scattering obstacle in normal electronic transport.[23] We show in Sec. V that the phase discontinuity arises in part from an unusual scattering process, where the presence of an impurity generates Andreev reflections instead of the usual normal reflections. Since the superfluid flow closes the normal reflection channel for energies near the band edge, it forces quasielectrons incident from the superconductor near the band edge to Andreev reflect as quasiholes, rather than normally reflect as quasielectrons, as illustrated in Fig. 2. Closing of the normal reflection channel near the gap edge under a superfluid flow has also been noted by Sanchez Cañizares and Sols.[12] This unusual type of Andreev reflection in an SIS junction is necessary to obtain the well-known step change in the order-parameter phase across a superconducting tunnel junction as we show in Sec. V.

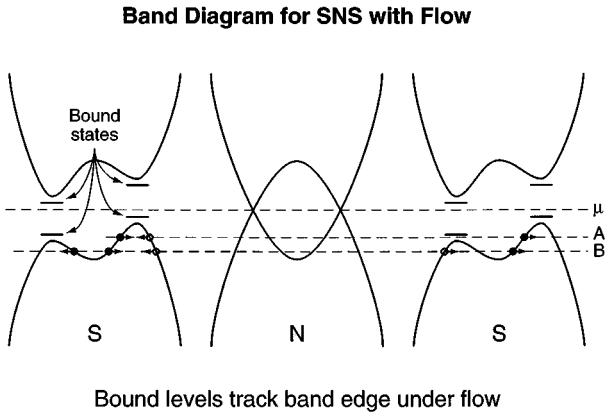

FIG. 2. Energy band diagram for an SNS junction. The energy bands in each superconductor ''tilt'' under a superfluid flow, and the bound-state energy levels track these band edges. Two different types of scattering states, labeled A and B, are shown incident from the left superconductor. Due to the superfluid flow, the normal reflection channel is closed for the scattering state near the band edge at energy A.

II. SUPERFLUID FLOW AND CURRENT CONSERVATION

To calculate motion of quasiparticles in the SNS junction, we use the Bogoliubov–de Gennes (BdG) equation

$$\begin{pmatrix} H(x)-\mu & \Delta(x) \\ \Delta^*(x) & -[H^*(x)-\mu] \end{pmatrix} \begin{pmatrix} u_n(x) \\ v_n(x) \end{pmatrix} = E_n \begin{pmatrix} u_n(x) \\ v_n(x) \end{pmatrix}, \tag{1}$$

where the one-electron Hamiltonian $H(x)$ is

$$H(x) = -\frac{\hbar^2}{2m}\frac{d^2}{dx^2} + V(x). \tag{2}$$

The electrostatic potential is $V(x)$. Because the SNS junction is in equilibrium, we fill the energy bands with quasiparticles according to the Fermi occupation factor

$$f(E_n)=\frac{1}{1+e^{E_n/k_BT}}. \tag{3}$$

The electrical current $J_Q(x)$ we compute from Refs. 14–18

$$J_Q=\sum_n [J_{u_n}+J_{v_n}]f(E_n)-\sum_n J_{v_n}. \tag{4}$$

The J_u and J_v are the Schrödinger currents associated with the waves u_n and v_n, namely, $J_{u_n}=(\hbar/m)\mathrm{Im}[u_n^*\nabla u_n]$ and $J_{v_n}=(\hbar/m)\mathrm{Im}[v_n^*\nabla v_n]$.

The BdG equation is derived from a self-consistent mean-field theory, and therefore requires the ordering parameter to be calculated self-consistently, as[25,26]

$$\Delta(x)=g(x)\sum_n f(E_n)v_n^*(x)u_n(x)\theta(\hbar\omega_D-|E_n|). \tag{5}$$

In contrast to the self-consistent Hartree potential from ordinary electrical conduction, failure to calculate the ordering parameter $\Delta(x)$ self-consistently will violate electrical current conservation in an inhomogeneous superconductor[14–18] leaving $\nabla J_Q\neq 0$. To actually evaluate Eq. (5), we cut off the summations for $|E_n|>\hbar\omega_D$, where ω_D is the Debye frequency.

We construct a scattering theory for the electrical current in the SNS junction following Refs. 3 and 6. Consider the band diagram for a superconductor shown in Fig. 2. The superconducting contact injects scattering states denoted by a wave vector k and band index α, so that the quantum number $n=(k,\alpha)$. One can work directly with the eigenstates of Eq. (1) when calculating superconducting properties,[26] including those with $E_n<0$. Our calculation differs from Refs. 3 and 6 because the energy bands are now ''tilted'' in the presence of a superfluid flow velocity v_s (Ref. 14) as shown in Fig. 2. This superfluid flow arises from a collective (center of mass) motion of quasiparticles, driven by a pairing potential of the form $\Delta(x)=|\Delta|\exp(2iqx+i\phi)$. The superfluid flow velocity is $v_s=\hbar q/m$, produced by a shift in the center of momentum $\hbar q$ along the x direction. Andreev reflections at a normal-metal–superconductor interface require such a superfluid flow in the superconductor to conserve electrical current.

To compute the self-consistent solutions to both Eqs. (1) and (5), we assume an initial guess $\Delta_0(x)$ for the ordering parameter, so that $\Delta(x)=\Delta_0(x)$ in Eq. (1). We then compute the corresponding solutions $u_n^0(x)$, $v_n^0(x)$, and E_n^0 of Eq. (1). Equation (5) then generates our next iterative guess for the ordering parameter $\Delta_1(x)$ as

$$\Delta_1(x)=g(x)\sum_n f(E_n^0)v_n^{0*}(x)u_n^0(x)\theta(\hbar\omega_D-|E_n^0|). \tag{6}$$

This new ordering parameter $\Delta_1(x)$ is then used to compute $u_n^1(x)$, $v_n^1(x)$, E_n^1, etc. We continue this procedure until the order parameter does not significantly vary between one iteration and the next.

Starting from our initial guess for $\Delta_0(x)$, the entire simulation proceeds to self-consistency on its own. The final current J_Q which results upon attaining the self-consistent solution, however, is unknown when choosing $\Delta_0(x)$. Although we could have enforced additional boundary conditions on the order parameter that would maintain a fixed current J_Q during each iteration, we found this unnecessary. To do the actual computations in this paper, we used both a scattering matrix method and direct diagonalization of Eq. (1), described in Appendix A.

III. ORDERING PARAMETER OF A BALLISTIC SNS JUNCTION

We assume a BCS coupling constant of the form

$$g(x)=\begin{cases}-1, & x<-L/2\\ 0, & -L/2<x<L/2\\ -1, & x>L/2,\end{cases} \tag{7}$$

so that the region between $-L/2<x<L/2$ is a normal conductor. The electron-phonon coupling constant $g(x)$ remains fixed throughout the calculation, as does the electrostatic potential which we take to be $V(x)=0$. As our initial guess for $\Delta_0(x)$, we assume

$$\Delta_0(x)=\begin{cases}\Delta_0 e^{2iqx}e^{i\phi_L}, & x<-L/2\\ 0, & -L/2<x<L/2\\ \Delta_0 e^{2iqx}e^{i\phi_R}, & x>L/2.\end{cases} \tag{8}$$

The total phase difference across the normal region in Eq. (8) is $\phi_R-\phi_L+2qL$.

To obtain information about superconducting correlations in the normal region we introduce the pairing correlation function $F(x)$, where

$$\Delta(x)=g(x)F(x). \tag{9}$$

That $F(x)$ is nonzero inside a normal region is equivalent to saying that Andreev reflections exist at the normal-metal–superconductor interfaces, and that these Andreev-reflected quasiparticles maintain their phase coherence inside the normal region. Both the order parameter

$$\Delta(x)=|\Delta(x)|e^{i\phi(x)} \tag{10}$$

and pair correlation function

$$F(x)=|F(x)|e^{i\phi(x)} \tag{11}$$

are typically represented by their magnitude and phase angle. Since we take $g(x)$ to be a real number throughout this paper, $\phi(x)$ is the phase angle of both $F(x)$ and $\Delta(x)$.

We show the resulting magnitude and phase of the self-consistent order parameter in a ballistic SNS junction carrying a supercurrent in Fig. 3. The superfluid flow velocity is half of the depairing velocity, $v_s=v_d/2$ where $v_d=|\Delta|/p_F$. The phase angle $\phi(x)$ increases linearly with position throughout the ballistic SNS junction, reminiscent of a uniform superconducting wire carrying a supercurrent. To compute $\Delta(x)$ in Fig. 3, we initially assumed $\phi_L-\phi_R=0$ from Eq. (8). The order-parameter phase gradient $d\phi/dx=2q$ remains unchanged during the iterative process, and the magnitude $|\Delta(x)|$ converges in about 15 iterations in Fig. 3.

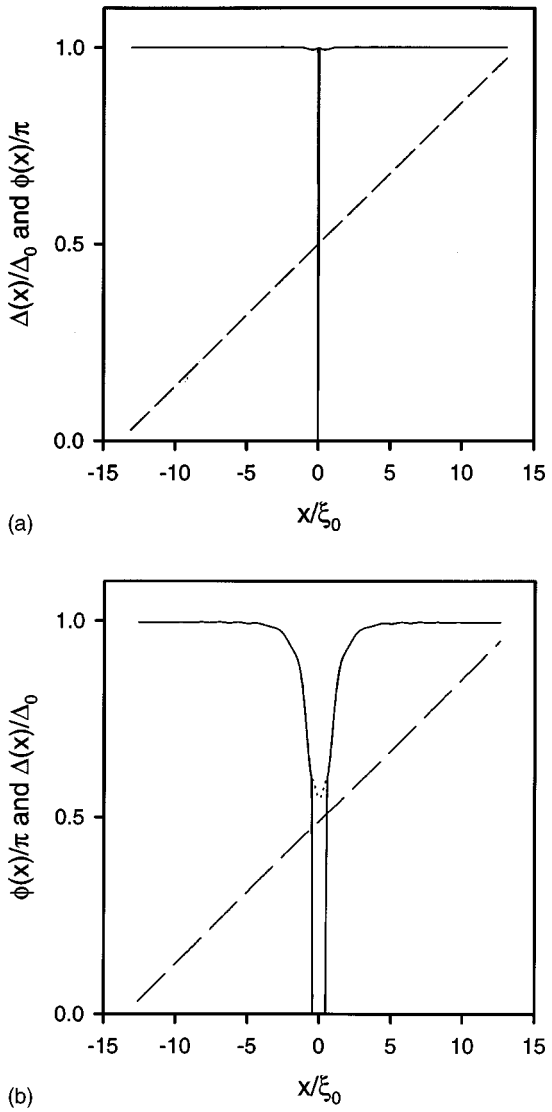

FIG. 3. Magnitude $|\Delta(x)|$ (solid) and phase $\phi(x)$ (dashed) of the self-consistent ordering parameter in a ballistic SNS junction. The superfluid flow velocity is half the Landau depairing velocity, $v_s = 0.5 v_d$. The length L of the normal region is (a) short ($L = 0.01\xi_0$), and (b) long ($L = \xi_0$). The order-parameter phase gradient is constant throughout the SNS junction.

For the short SNS junction having $L \ll \xi_0$ in Fig. 3(a), the magnitude of the order parameter is only slightly changed from our initial guess. If we had taken $L = 0$, our initial guess would in fact be the correct self-consistent solution for the order parameter. The magnitude $|\Delta(x)|$ however, is reduced near the normal-metal–superconductor interfaces, especially for the longer SNS junction of Fig. 3(b). Similar results in the absence of a supercurrent flow were obtained in Ref. 27. A nonzero pairing correlation function $|F(x)|$ exists inside the normal region, shown by the dotted line in Fig. 3(b).

The final self-consistent order parameter for a ballistic SNS junction (shown in Fig. 3) has a uniform phase gradient, independent of the initial guess for $\Delta_0(x)$. Figure 4 follows the self-consistent evolution of the pair potential $\Delta_n(x)$ for a step change in the phase $\phi_0(x)$. We therefore take $q = 0$ and $\phi_L - \phi_R \neq 0$ in Eq. (8). The phase angle evolves from a step discontinuity to a uniform phase gradient in about 140 iterations in Fig. 4. Clearly the initial guess $\Delta_0(x) = |\Delta_0| \exp(2iqx)$ in Fig. 3 converges more rapidly to self-consistency for the ballistic SNS junction. This should have been expected, since the ballistic SNS junction indeed strongly resembles a superconducting wire.

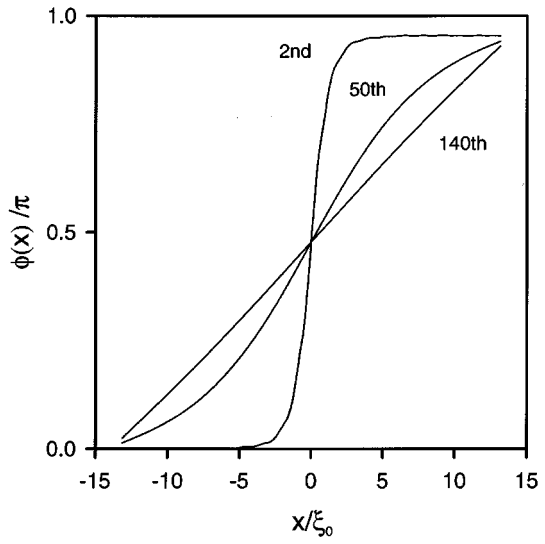

FIG. 4. Self-consistent evolution of the order-parameter phase angle $\phi_n(x)$ for the short junction of Fig. 2. The final self-consistent phase angle varies linearly with position, even if the initial guess for $\phi_0(x)$ is a step discontinuity. $\phi_n(x)$ converges from the step discontinuity to the linear function assumed in Fig. 2 in about 140 iterations.

Figure 5 shows the spatial variation of the current $J_Q(x)$ as a function of iteration number. In Fig. 5(a), the step-change model for $\phi_0(x)$, the current is initially localized in the normal region of the SNS junction and is carried by Andreev bound states. The current $J_Q^0(x)$ corresponding to our initial guess for $\Delta_0(x)$ decays to zero inside the superconductors, violating current conservation. As the iteration procedure continues, the current becomes extended throughout space and is constant with position. It is therefore not necessary to invoke an *ad hoc* ''source term'' to obtain current conservation, as done in Ref. 28. Once self-consistency is reached, the spatially extended current flowing inside an SNS junction is carried solely by the continuum energy levels, not the bound levels (as predicted by a non-self-consistent calculation). Figure 5(b), the linear phase change model for $\phi_0(x)$, converges to the same constant current value in fewer iterations. Appendix B constructs an analytical proof explaining why the bound levels carry no net current in the uniform-width SNS junction.

To obtain these results using the finite-element method in Appendix A, it is necessary for the phase $\phi(x)$ in each element to vary linearly with position. A piecewise constant model for the phase $\phi(x)$ does not permit any supercurrent flow in the element, forcing the self-consistent scheme towards zero current. Physically, it is impossible to construct a supercurrent carrying wire from finite elements, each of which cannot carry a supercurrent. One can still employ a piecewise constant model for magnitude of the order parameter without violating any basic physical principles.

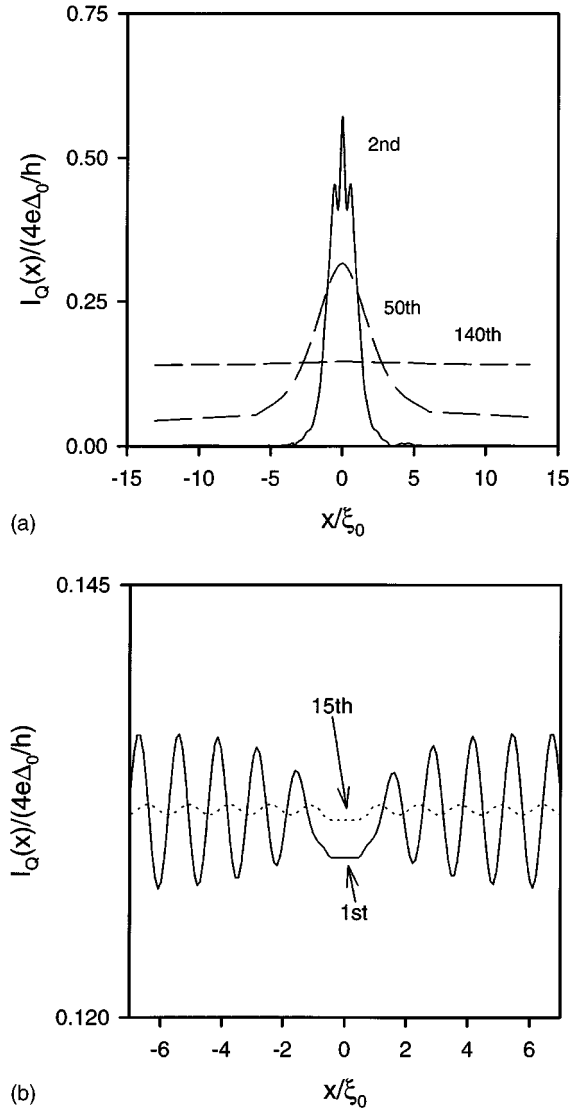

FIG. 5. Electrical current $J_Q(x)$ as a function of iteration number for the short junction of Fig. 2. The initial guess for the phase $\phi_0(x)$ is either (a) the step-change model or (b) the linear phase model. Current conservation occurs when the iterative scheme reaches self-consistency. The final self-consistent electrical current flows through spatially extended states, instead of through the bound levels predicted in a non-self-consistent calculation.

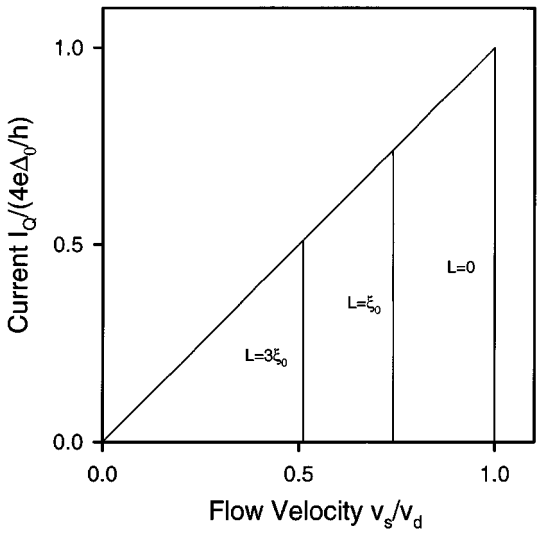

FIG. 6. Electrical current flow in an SNS junction where the length of the normal region is $L=0$, $L=\xi_0$, $L=3\xi_0$. The current increases linearly with the superfluid flow velocity as $I=env_s$. The critical depairing velocity decreases as the length of the normal region increases.

IV. CRITICAL CURRENT OF A BALLISTIC SNS JUNCTION

In a superconducting wire the phase gradient $2q$ is directly related to the current by $I=env_s$, where $v_s=\hbar q/m$. Section III demonstrates that phase gradient of the pair-correlation function is constant in a ballistic SNS junction. Since inserting the normal region does not disturb the phase gradient of the pair-correlation function, the current of an SNS junction embedded in a long superconducting wire is also $I=env_s$. As long as the electron density does not vary with position x, we will have $I=env_s$ in a ballistic SNS junction independent of the exact form of the electron-phonon coupling $g(x)$. The critical current is then defined by the largest value of q for which a solution to Eq. (5) exists.

Figure 6 shows the critical current as a function of superfluid flow velocity v_s for various lengths L of the normal region. The supercurrent increases linearly with flow velocity, just as for a one-dimensional (1D) superconducting wire. When $L=0$, the critical current is the same as for a 1D superconducting wire, namely, $I_c=4e|\Delta|/h$, for the same reasons as given in Ref. 14. The abrupt collapse of the supercurrent when $v_s=v_d=\Delta/p_F$ occurs in a 1D superconducting wire when the superfluid flow velocity forces the quasiparticle energy gap to close.

The critical current of an SNS junction having $L>0$ is smaller than for a superconducting wire in Fig. 6 because the lowest energy Andreev bound level[21,22] in the SNS junction is less than the bulk energy gap, i.e., $E_0\leqslant\Delta$. The critical current is reached when the lowest energy Andreev bound level aligns with the Fermi level, closing the effective quasiparticle energy gap. The critical superfluid velocity in Fig. 6 we find then given by $v_s=v_c=E_0/p_F$. Since the bound levels lie deeper inside the energy gap for a longer normal region, E_0 decreases as the length of the normal region increases. Figure 6 also shows the corresponding maximum superfluid flow velocity $v_c\leqslant v_d$ decreases with increasing length L of the normal region.

No self-consistent solution for the order parameter from Eq. (5) exists at zero voltage when the superfluid velocity exceeds the small critical velocity $v_s>v_c$. However, this does not necessarily imply the order parameter in the narrow superconductor collapses when one exceeds the critical current. A voltage will likely develop in the SNS junction, allowing superconductivity to persist in the narrow region until the superfluid velocity exceeds Landau's depairing velocity, $v_s>v_d$. Confirming the appearance of this finite voltage is beyond the scope of this paper.

One can estimate the critical current I_c using the approximate bound energy levels E_n of Refs. 21 and 22. For a long SNS junction ($L\gg\xi_0$) in the absence of a superfluid flow, the energy levels are

$$E_n \simeq \Delta \frac{\xi_0}{L+2\xi_0}\left[2\pi\left(n+\frac{1}{2}\right) \pm (\phi_R - \phi_L)\right]. \quad (12)$$

The BCS healing length is $\xi_0 = \hbar v_F / 2\Delta$. The bound levels of Eq. (12) form in the pair potential given by Eq. (8) with $q=0$. The bound level closest to the Fermi level is $n=0$, so that the lowest bound Andreev energy level in a long SNS junction ($L \gg \xi_0$) with $\phi_R - \phi_L = 0$ is

$$E_0 = \pi\Delta \frac{\xi_0}{L+2\xi_0}. \quad (13)$$

The bound levels E_n form from the extremum points of the energy bands near $k \simeq \pm k_F$. As the energy bands ''tilt'' under a superfluid flow, the bound levels (nearly) rigidly follow the band extrema (shown schematically in Fig. 2). If one indeed assumes the energy levels in Eq. (13) rigidly follow the band extrema under a superfluid flow, we have

$$E_0(v_s) \simeq E_0 - m v_F v_s. \quad (14)$$

The maximum superfluid velocity v_c in an SNS junction is set when one of these bound levels crosses the Fermi level, closing the quasiparticle energy gap. Setting $E_0(v_s)=0$ in Eq. (14), we obtain the critical superfluid velocity

$$v_c = \frac{E_0}{p_F}. \quad (15)$$

The critical current I_c is then approximately

$$I_c = e n v_c = e\left(\frac{4k_F}{2\pi}\right)\left(\frac{E_0}{p_F}\right). \quad (16)$$

Inserting Eq. (13) into Eq. (16), we obtain the critical current of a long ($L \gg \xi_0$) SNS junction as[3,5,6,8,19,22]

$$I_c \simeq \frac{4e\Delta}{h}\left(\frac{\pi\xi_0}{L+2\xi_0}\right) = \frac{e v_F}{L+2\xi_0}. \quad (17)$$

For a short SNS junction ($L \ll \xi_0$) Eq. (13) is modified to $E_0 \simeq \Delta$,[1] so that the critical current becomes

$$I_c \simeq \frac{4e\Delta}{h} = \frac{2}{\pi}\frac{e\Delta}{\hbar}. \quad (18)$$

Equation (18) is the same critical current predicted for a one-dimensional superconducting wire,[14,29] but is smaller than that of a superconducting point contact.[1]

Instead of estimating the critical current from a pairing potential which neglects superfluid flow, as done above, we can also obtain the Andreev energy levels from Eq. (8), taking explicit account of the superfluid flow. Under a superfluid flow, the BCS coherence factors $u_0(E)$ and $v_0(E)$ to lowest order in q are approximately shifted to an energy $E \rightarrow E \mp (\hbar^2 k q / m)$. The bound-state energy levels corresponding to the pair potential $\Delta_0(x)$ from Eq. (8) then satisfy the resonance condition

$$-2\cos^{-1}\left(\frac{E \mp m v_F v_s}{\Delta}\right) + k_F L\left(\frac{E}{\mu}\right) \mp (\phi_R - \phi_L) \mp 2qL = 2\pi n. \quad (19)$$

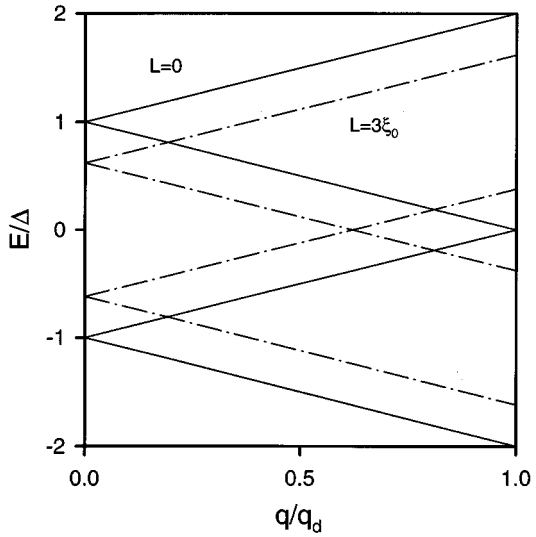

FIG. 7. Bound-state energy levels vs superfluid flow velocity, generated from the zeroth-order guess for $\Delta_0(x)$. The energy levels at $q=0$ are split by the superfluid flow, and rigidly follow the superconducting band edge as it shifts subject to the flow. The self-consistency condition can no longer be satisfied (at zero voltage) when one of these bound levels crosses the Fermi level. Uniform-width SNS junctions having length $L=3\xi_0$ (dashed), therefore carry a lower critical current than when $L=0$ (solid).

Note that the total phase difference across the normal region is $2qL + (\phi_R - \phi_L)$ in Eq. (19). The self-consistent calculation in Sec. III showed that $\phi_R - \phi_L = 0$.

The bound-state energies in an SNS junction as a function of the superfluid velocity v_s, generated from Eq. (19) with $\phi_R - \phi_L = 0$, are shown in Fig. 7. The doubly degenerate bound levels at $q=0$ are split by the superfluid flow. Imposing a superfluid flow lifts the degeneracy of the bound-energy levels because an electron-hole pair drifting with the superfluid flow velocity has a higher energy than an electron-hole pair drifting in the opposite direction from the superfluid velocity.

The depairing condition is approximately $v_s = v_c$ when $E=0$ in Eq. (19). Setting $\phi_R - \phi_L = 0$ for the ballistic SNS junction gives

$$-2\cos^{-1}(2\xi_0 q_c) - 2q_c L = 2\pi n. \quad (20)$$

The critical current I_c is then approximately

$$I_c = e n v_c = e\left(\frac{4k_F}{2\pi}\right)\left(\frac{\hbar q_c}{m}\right). \quad (21)$$

Combining Eqs. (20) and (21) gives Eq. (18) for a short junction and Eq. (17) for a long junction. Both methods of estimating the critical current give the same results. Note that, even though bound states crossing the Fermi level set the maximum superfluid velocity at which a self-consistent solution to Eq. (5) exists at zero voltage, and therefore set the critical current, the current itself is carried through continuum states outside the superconducting gap.

Equation (17) is the same critical current predicted in a non-self-consistent treatment of the long SNS junction.[3,6,22] However, Eq. (17) overestimates the actual critical current,

since the actual self-consistent order parameter is reduced and rounded near each NS boundary. This rounding of $\Delta(x)$ near the NS interface produces an effectively longer junction, with bound Andreev energy levels that lie closer to the Fermi level. A smaller superfluid flow velocity than that assumed in Eq. (17) will therefore leave Eq. (5) without a solution at zero voltage. Rounding of the order parameter has been quantified by Plehn, Gunsenheimer, and Kümmel[20] using an effective electrical length $L^* \geqslant L$, namely,

$$L^* = \int_{-\infty}^{\infty} \left[1 - \frac{\Delta(x)}{\Delta_0} \right] dx. \tag{22}$$

Equation (17) still describes the critical current in an SNS junction subject to rounding of the order parameter, provided we replace $L \rightarrow L^*$.

V. ORDERING PARAMETER IN AN SIS TUNNEL JUNCTION

In a ballistic SNS junction, quasielectrons incident from one superconductor transmit to the other superconductor with a probability close to unity. This cannot be true in an SIS junction, where a tunnel barrier will normally reflect the electrons. Such normal reflection is shown as the type-''B'' scattering process in Fig. 2. But the superfluid flow in a uniform width SIS junction, which must develop in the leads to ensure current conservation, closes the normal reflection channel near the superconducting gap edge as shown in Fig. 2. Normal reflection of quasielectrons back into the superconductor is therefore impossible. Since the electrons cannot easily transmit through the insulating barrier, the only possible remaining scattering process is reflection back into the superconductor as a quasihole. This unusual type of ''Andreev reflection'' back into the superconductor, due to the presence of an impurity, is shown as the type-''*A*'' scattering process in Fig. 2. We show in this section that this unusual ''type-A'' Andreev reflection, due to the presence of the insulator, is important to determine the self-consistent order parameter in a uniform-width SIS junction.

Figure 8 shows the reflection coefficients for electronlike quasiparticles incident from the left superconductor on an SIS junction. Both the A- and B-type processes from Fig. 2, also shown schematically in Fig. 8, can be clearly identified in the quasiparticle reflection coefficients. As the normal reflection channel begins to close, the (particle current) normal reflection coefficient R_n decreases and the Andreev reflection coefficient R_a begins to increase. Since transmission through the tunnel barier is small, $T=0.01$, we have $R_a+R_n \simeq 1$. When the normal reflection channel is closed, Andreev reflection of a quasielectron back into the superconductor as a quasihole is a two-step process involving the normal reflection of both an electron and hole from the impurity as shown in Fig. 8.

The final self-consistent order parameter we find for the SIS junction is similar to the one assumed in standard tunneling theory.[30] Figure 9 shows a self-consistent calculation of the order parameter in an SIS structure. The current $I=0.4I_{AB}$, where $I_{AB}=eT\Delta/2\hbar$ is the Ambegaokar-Baratoff critical current.[30] The barrier transmission in Fig. 9 is $T \simeq 0.01$. A discontinuity in the order-parameter phase arises

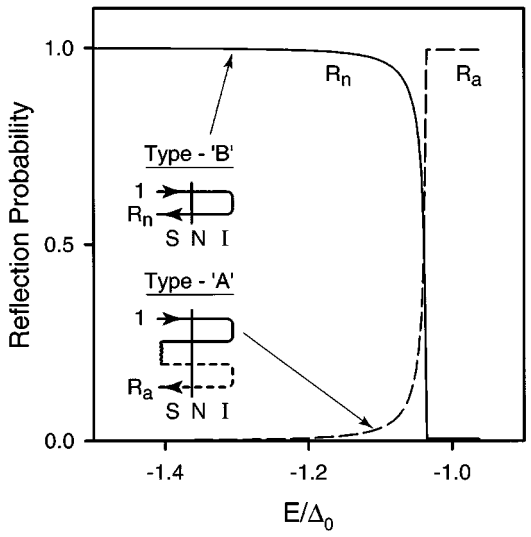

FIG. 8. Particle current reflection coefficients for both normal (R_n) and Andreev (R_a) type processes in an SIS junction. The energy bands are subject to a superfluid flow as indicated in Fig. 1, so that the normal reflection channel is cut off for energies close to the superconducting gap.

across the tunneling barrier due to a current flow, as commonly assumed in tunneling theory.[30] A small superfluid flow inside the superconducting regions, approximately $v_s \simeq I_{AB}\sin\theta/en$, maintains current conservation throughout the structure.

The final self-consistent order parameter in Fig. 9 has a discontinuity in its phase across the impurity. Figure 10 shows the self-consistent development the order-parameter phase $\phi(x)$ as a function of iteration number. Rather than assume a phase discontinuity across the impurity, we start with a small supercurrent flow and allow the phase differ-

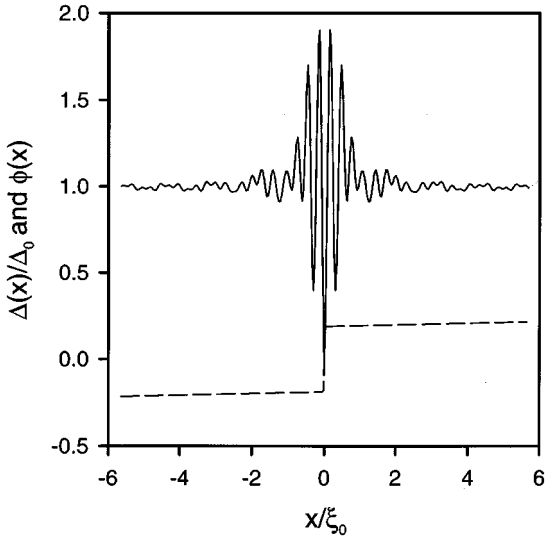

FIG. 9. Self-consistent magnitude (solid) and phase (dashed) of the order parameter $\Delta(x)$ in an SIS junction. A small superfluid flow supports the phase discontinuity in the order parameter at $x=0$. That the magnitude of $|\Delta(x)|$ is not constant is an artifact of a local model for the electron-phonon interaction.

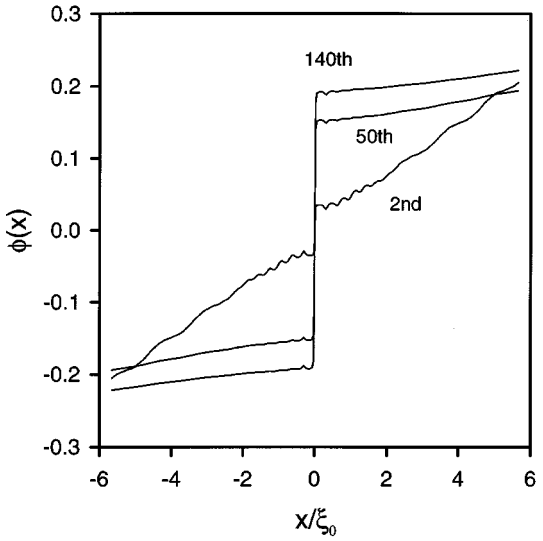

FIG. 10. The final self-consistent order-parameter phase angle in an SIS junction has a step discontinuity across the impurity, even if the initial guess $\phi_0(x)$ assumes only a uniform superfluid flow. An initial guess for the ordering parameter having a linear phase gradient converges to a steplike phase discontinuity across the impurity in about 140 iterations. The small superfluid flow in the superconductors assumed in Fig. 8 is also present.

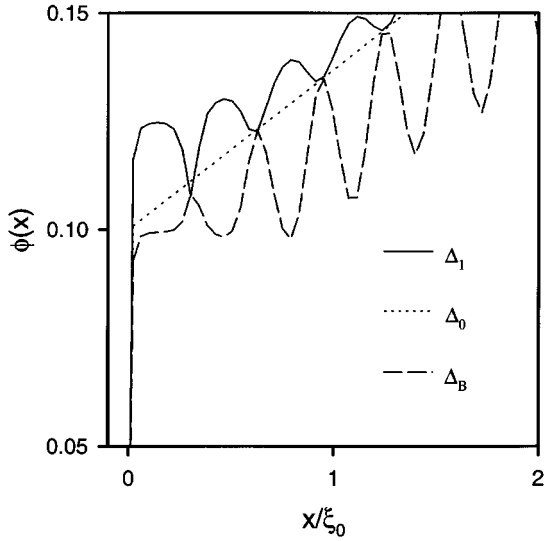

FIG. 11. For the order-parameter phase discontinuity in an SIS junction (at $x=0$) to converge to its final self-consistent value requires unusual Andreev reflection (type-A) processes. Including only the processes for which the normal reflection channel is open (type-B processes) will not force the order parameter towards its final self-consistent value. Only adding both processes, so that $\Delta_1=\Delta_A+\Delta_B$, forces the order parameter towards convergence.

ence to develop naturally from Eq. (5). About 140 iterations are required to reach the self-consistent solution in Fig. 10. In contrast, Fig. 9 assumes both a step change in the order parameter phase across the impurity and a small superfluid flow as the initial guess for $\phi_0(x)$. Figure 9 converges to the same result as Fig. 10 in about 20 iterations.

The unusual type-A Andreev reflection processes are essential to the phase discontinuity in an SIS junction developing its final self-consistent value. Figure 11 shows an initial guess Δ_0 for the phase discontinuity, which is much less than its final self-consistent value in Fig. 9. We can split the integral equation (6) for $\Delta_1(x)$ into two energy regions and write $\Delta_1=\Delta_A+\Delta_B$. Here the energies $|E|<\Delta+\hbar^2kq/m$ describe mostly type-A processes, and energies $|E|>\Delta+\hbar^2kq/m$ contain mostly type-B reflection processes. Figure 11 shows that including only type-B processes in Eq. (6) reduces the phase discontinuity. Adding the type-A processes forces $\Delta_1(x)$ towards its final self-consistent value. This is reasonable, as only Andreev reflections can induce the required superfluid flow inside the superconducting leads.

The order-parameter magnitude $|\Delta(x)|$ in Fig. 9 also displays unphysical oscillations, having a spatial period of half the Fermi wavelength.[11,24] These unphysical oscillations in $|\Delta(x)|$ for the SIS junction (or indeed when any normal reflections are present inside a superconductor) suggest that disordered superconductors must be treated using a full nonlocal theory of the electron-phonon interaction. The oscillations in $|\Delta(x)|$ are present even without a current flow,[24] and have the same spatial period as the Friedel oscillations of the charge density in a normal metal. The oscillations in $|\Delta(x)|$ arise from interference between the incident and normally reflected quasiparticles near the Fermi surface. In ordinary high-density superconductors where $\xi_0 \gg \lambda_F$, the oscillations in $|\Delta(x)|$ will be averaged away by the nonlocal electron-phonon interaction. However, oscillations in $|\Delta(x)|$ are speculated to possibly appear in high-T_c SIS junctions,[24] since the Fermi wavelength and coherence length are comparable. Proving or disproving this speculation will require further calculation.

The oscillations in $|\Delta(x)|$ damp out over a distance corresponding to the Debye frequency, namely, $L_{nl}=\hbar v_F/(\hbar\omega_D-\Delta)$, since they are Fourier synthesized from wave vectors lying within an energy range $\hbar\omega_D-\Delta$ near the Fermi level. This ''nonlocality'' distance L_{nl} is the length scale within which the quasiparticle wave functions near a point x would contribute to the spatially varying order parameter $\Delta(x)$ in a nonlocal theory of superconductivity. The theory of Sec. II makes only the usual local approximation for the superconducting order parameter in Eq. (5).

To understand the origin of the oscillations of the order parameter magnitude $|\Delta(x)|$ in Fig. 9, we can initially guess a constant order parameter Δ_0. We then construct an approximate first-order solution $\Delta_1(x)$ assuming the barrier transmission is zero, and there is no superfluid flow ($q=0$). These assumptions correspond to zero current flow through the SIS junction. We find

$$\Delta_1 \simeq \Delta_0 - \cos(2k_Fx)g\int_{\Delta_0}^{\hbar\omega_D} N(E)u_0v_0^*\cos(Ex/|\Delta_0|\xi_0)dE. \tag{23}$$

The oscillations in Fig. 9 come from the $\cos(2k_Fx)$ term. Equation (23) can be approximated near $x=0$ to describe the central peak in $|\Delta(x)|$ in Fig. 9 as

$$\Delta_1 \simeq \Delta_0[1-\cos(2k_Fx)\mathrm{sinc}\{2(\hbar\omega_D-\Delta_0)x/\hbar v_F\}]. \tag{24}$$

Equation (24) indeed decays over the nonlocality length $L_{\rm nl}=\hbar v_F/2(\hbar\omega_D-\Delta)$.

Any features in $\Delta(x)$ appearing on a length scale smaller than the nonlocality length $L_{\rm nl}$ cannot be taken seriously unless one solves a nonlocal version of the BdG equation.[31] We actually expect $|\Delta(x)|$ to be constant in a nonlocal calculation of the order parameter in an SIS junction, so long as $\lambda_F<L_{\rm nl}$. Naively, one could view a nonlocal order parameter as averaging the local one over a length scale $L_{\rm nl}$, removing any oscillations on smaller length scales. If they exist, the best chance of observing such oscillations in the superconducting order parameter for an SIS junction would be in a low-density superconductor where the inequality $\lambda_F\gg L_{\rm nl}$ might be satisfied. A calculation valid for this parameter regime remains to be done.

VI. CONCLUSIONS

We have calculated the electrical current and self-consistent order parameter for a normal region embedded in a superconducting wire, where all regions of the SNS junction have equal widths. In this uniform-width ballistic SNS junction, the phase gradient of the pair-correlation function is constant in space and the current is carried by spatially extended continuum states. Andreev-bound levels carry no net current in a ballistic SNS junction having a constant width. This is in contrast to an SNS junction embedded in a point contact, where there is a fixed phase discontinuity across the normal region and the current is carried by Andreev bound levels.

Even though the energy distribution of the electrical current is quite different in a uniform-width SNS junction vs an SNS point contact, the critical current for both types of junctions is still given by $I_c=ev_F/(L+2\xi_0)$ at zero temperature. The main difference between the two junction types is that the physical and effective electrical junction lengths are different for a uniform-width SNS junction. The superconducting order-parameter magnitude is reduced near the NS boundaries in this uniform-width SNS junction, especially when the normal region is longer than the coherence length, $L\gg\xi_0$. Rounding of the order parameter at the NS interface occurs because a smaller number of states are available near the NS boundary in a uniform width SNS junction compared to the SNS point contact. This rounding of the order parameter at the NS interfaces increases the effective electrical length L^* of the junction as found in Ref. 20, so that $L^*\geqslant L$. The corresponding critical current at zero temperature is reduced to $I_c=ev_F/(L^*+2\xi_0)$. The difference in the energy distribution of the currents between point contact and uniform-width SNS junctions may also lead to a different temperature dependence of their critical currents.

We have also calculated the self-consistent order-parameter magnitude and phase for a tunnel barrier placed inside the normal region of a uniform-width SNS junction. The resulting discontinuity in the order-parameter phase, appearing across the insulator of the current-carrying uniform-width SIS junction, depends on an unusual type of Andreev reflection due to the presence of an impurity. The superfluid flow closes the normal reflection channel for quasiparticles injected near the band edge, leaving only the Andreev reflection channel open. Developing a phase discontinuity across the insulator requires this unusual type of Andreev reflection due to the insulator. If one further desires to obtain the correct order parameter magnitude, it is necessary to include the full nonlocal electron-phonon interaction (instead of the usual local-phonon approximation). Obtaining the self-consistent order-parameter magnitude requires a nonlocal theory of the electron-phonon interaction whenever electrostatic potentials $V(x)$ producing normal reflections are present inside a superconductor.

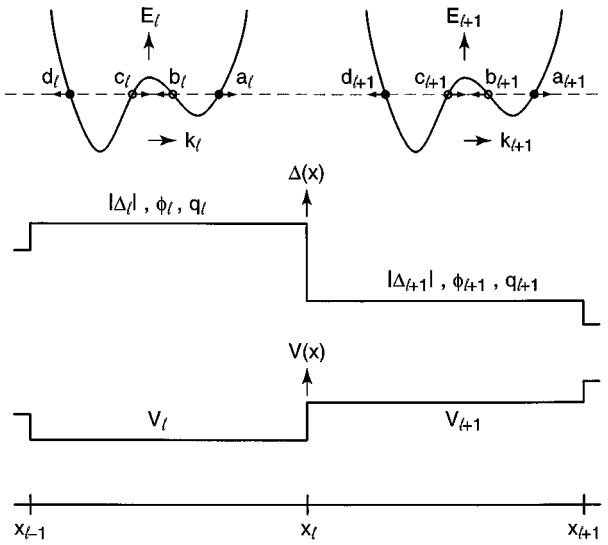

FIG. 12. Scattering states on the energy bands for two adjacent superconducting regions. The order parameter magnitude ($|\Delta_l|$), phase (ϕ_l), and flow velocity (q_l) are needed to describe each superconducting region. The electrostatic potential (V_l) can also vary with position.

ACKNOWLEDGMENTS

We thank Supriyo Datta and Albert Overhauser for useful discussions. We gratefully acknowledge financial support from the David and Lucile Packard Foundation.

APPENDIX A: NUMERICAL SOLUTION OF THE BdG EQUATIONS

Finding a self-consistent solution to the BdG equations almost always requires numerical solution methods. We used two different methods described below; direct diagonalization and a scattering matrix method, to obtain the results in this paper. Each method provided a numerical check on the other, and both gave identical numerical results.

We discretize the one-dimensional space as shown in Fig. 12. In each region the order parameter is

$$\Delta_l(x)=|\Delta_l|\exp i(2q_lx+\phi_l)=|\Delta_l(x)|e^{i\phi_l(x)}, \qquad \text{(A1)}$$

where $x_{l-1}<x<x_l$. The potential $V_l(x)=V_l$ and the BCS coupling constant $g_l(x)=g_l$ are also constant in each region. The quasiparticle wave functions in each region are then given by

$$\psi_l(x)=\begin{bmatrix}u_l(x)\\ v_l(x)\end{bmatrix}=a_l\begin{bmatrix}U_{al}e^{iq_lx}e^{i\phi_l/2}\\ V_{al}e^{-iq_lx}e^{-i\phi_l/2}\end{bmatrix}e^{ik_{al}x}+b_l\begin{bmatrix}V_{bl}e^{iq_lx}e^{i\phi_l/2}\\ U_{bl}e^{-iq_lx}e^{-i\phi_l/2}\end{bmatrix}e^{ik_{bl}x}+c_l\begin{bmatrix}V_{cl}e^{iq_lx}e^{i\phi_l/2}\\ U_{cl}e^{-iq_lx}e^{-i\phi_l/2}\end{bmatrix}e^{-ik_{cl}x}+d_l\begin{bmatrix}U_{dl}e^{iq_lx}e^{i\phi_l/2}\\ V_{dl}e^{-iq_lx}e^{-i\phi_l/2}\end{bmatrix}e^{-ik_{dl}x}. \tag{A2}$$

The wave vectors $k_{al},k_{bl},k_{cl},k_{dl}$ for each energy E are found[32] from the quartic equation

$$k^4-2k^2\left(k_F^2+q_l^2-\frac{2mV_l}{\hbar^2}\right)+4kq_l\left(\frac{2mE}{\hbar^2}\right)+\left(q_l^2-k_F^2+\frac{2mV_l}{\hbar^2}\right)^2+\left(\frac{2m|\Delta_l|}{\hbar^2}\right)^2-\left(\frac{2mE}{\hbar^2}\right)^2=0. \tag{A3}$$

Equation (A3) follows from the dispersion law in a uniform superconductor having a constant q_l, $|\Delta_l|$, and V_l, namely,

$$E=(\hbar k)(\hbar q_l/m)\pm\sqrt{E_{Al}^2+|\Delta_l|^2}, \tag{A4}$$

where the ''center of mass'' energy E_A in each region is

$$E_{Al}(k,q_l)=\frac{\hbar^2k^2}{2m}+\frac{\hbar^2q_l^2}{2m}+V_l-\mu. \tag{A5}$$

The coherence factors U and V when the conductor is subject to a superfluid flow are

$$U_l=\frac{A_l}{\sqrt{|A_l|^2+|B_l|^2}} \tag{A6}$$

and

$$V_l=\frac{B_l}{\sqrt{|A_l|^2+|B_l|^2}}. \tag{A7}$$

The factors A and B are

$$A_l^2=\frac{1}{2}\left[1+\frac{E_{Al}}{\sqrt{E_{Al}^2+|\Delta_l|^2}}\right], \tag{A8}$$

$$B_l^2=\frac{1}{2}\left[1-\frac{E_{Al}}{\sqrt{E_{Al}^2+|\Delta_l|^2}}\right], \tag{A9}$$

and are different for each state a,b,c,d.

At each boundary we enforce continuity of the wave function and its derivative at $x=x_{l+1}$ according to

$$\psi_l(x=x_l)=\psi_{l+1}(x=x_l) \tag{A10}$$

and

$$\left.\frac{\partial\psi_l}{\partial x}\right|_{x=x_l}=\left.\frac{\partial\psi_{l+1}}{\partial x}\right|_{x=x_l}. \tag{A11}$$

Equations (A10) and (A11) enforce relations between the wave function amplitudes a,b,c,d in different regions, namely, at $x=x_l$

$$M^l(x_l)\begin{bmatrix}a_l\\ b_l\\ c_l\\ d_l\end{bmatrix}=M^{l+1}(x_l)\begin{bmatrix}a_{l+1}\\ b_{l+1}\\ c_{l+1}\\ d_{l+1}\end{bmatrix}. \tag{A12}$$

The first (second) row of Eq. (A12) enforces continuity of $u(x)$ $[v(x)]$. The third (fourth) row of Eq. (A12) enforces continuity of $du(x)/dx$ $[dv(x)/dx]$. The matrix $M_l(x)$ is therefore

$M^l(x)$

$$=\begin{bmatrix}
e^{iq_lx}e^{i\phi_l/2}e^{ik_{a,l}x}U_{a,l} & e^{iq_lx}e^{i\phi_l/2}e^{ik_{b,l}x}V_{b,l} & e^{iq_lx}e^{i\phi_l/2}e^{-ik_{c,l}x}V_{c,l} & e^{iq_lx}e^{i\phi_l/2}e^{-ik_{d,l}x}U_{d,l}\\
e^{-iq_lx}e^{-i\phi_l/2}e^{ik_{a,l}x}V_{a,l} & e^{-iq_lx}e^{-i\phi_l/2}e^{ik_{b,l}x}U_{b,l} & e^{-iq_lx}e^{-i\phi_l/2}e^{-ik_{c,l}x}U_{c,l} & e^{-iq_lx}e^{-i\phi_l/2}e^{-ik_{d,l}x}V_{d,l}\\
i(q_l+k_{a,l})e^{iq_lx}e^{i\phi_l/2}e^{ik_{a,l}x}U_{a,l} & i(q_l+k_{b,l})e^{iq_lx}e^{i\phi_l/2}e^{ik_{b,l}x}V_{b,l} & i(q_l-k_{c,l})e^{iq_lx}e^{i\phi_l/2}e^{-ik_{c,l}x}V_{c,l} & i(q_l+k_{a,l})e^{iq_lx}e^{i\phi_l/2}e^{-ik_{d,l}x}U_{d,l}\\
i(-q_l+k_{a,l})e^{-iq_lx}e^{-i\phi_l/2}e^{ik_{a,l}x}V_{a,l} & i(-q_l+k_{b,l})e^{-iq_lx}e^{-i\phi_l/2}e^{ik_{b,l}x}U_{b,l} & i(-q_l-k_{c,l})e^{-iq_lx}e^{-i\phi_l/2}e^{-ik_{c,l}x}U_{c,l} & i(-q_l+k_{a,l})e^{-iq_lx}e^{-i\phi_l/2}e^{-ik_{d,l}x}V_{d,l}
\end{bmatrix}. \tag{A13}$$

1. Direct diagonalization method

Consider an electronlike quasiparticle incident from the left upon a piece of superconducting material divided into only three regions. The boundary conditions are then $a_1=1$, $c_1=0$, $d_3=0$, and $b_3=0$. These merely say that no holelike quasiparticles are incident from the left, and that no particles are incident from the right. Applying Eq. (A13) at the two boundaries, we obtain an 8×8 matrix to diagonalize for the scattered wave everywhere, namely,

$$\begin{bmatrix} M^1_{12}(x_1) & M^1_{14}(x_1) & -M^2_{11}(x_1) & -M^2_{12}(x_1) & -M^2_{13}(x_1) & -M^2_{14}(x_1) & 0 & 0 \\ M^1_{22}(x_1) & M^1_{24}(x_1) & -M^2_{21}(x_1) & -M^2_{22}(x_1) & -M^2_{23}(x_1) & -M^2_{24}(x_1) & 0 & 0 \\ M^1_{32}(x_1) & M^1_{34}(x_1) & -M^2_{31}(x_1) & -M^2_{32}(x_1) & -M^2_{33}(x_1) & -M^2_{34}(x_1) & 0 & 0 \\ M^1_{42}(x_1) & M^1_{44}(x_1) & -M^2_{41}(x_1) & -M^2_{42}(x_1) & -M^2_{43}(x_1) & -M^2_{44}(x_1) & 0 & 0 \\ 0 & 0 & M^2_{11}(x_2) & M^2_{12}(x_2) & M^2_{13}(x_2) & M^2_{14}(x_2) & -M^3_{11}(x_2) & -M^3_{13}(x_2) \\ 0 & 0 & M^2_{21}(x_2) & M^2_{22}(x_2) & M^2_{23}(x_2) & M^2_{24}(x_2) & -M^3_{21}(x_2) & -M^3_{23}(x_2) \\ 0 & 0 & M^2_{31}(x_2) & M^2_{32}(x_2) & M^2_{33}(x_2) & M^2_{34}(x_2) & -M^3_{31}(x_2) & -M^3_{33}(x_2) \\ 0 & 0 & M^2_{41}(x_2) & M^2_{42}(x_2) & M^2_{43}(x_2) & M^2_{44}(x_2) & -M^3_{41}(x_2) & -M^3_{43}(x_2) \end{bmatrix} \begin{bmatrix} b_1 \\ d_1 \\ a_2 \\ b_2 \\ c_2 \\ d_2 \\ a_3 \\ c_3 \end{bmatrix} = \begin{bmatrix} -M^1_{11}(x_1) \\ -M^1_{21}(x_1) \\ -M^1_{31}(x_1) \\ -M^1_{41}(x_1) \\ 0 \\ 0 \\ 0 \\ 0 \end{bmatrix}. \tag{A14}$$

For an inhomogeneous superconducting material divided into $m+1$ different regions, we repeatedly apply Eq. (A13) at the m boundaries. After applying the scattering boundary conditions, we obtain a matrix equation similar to Eq. (A14) of the form $[A][B]=[C]$. The $4m\times 4m$ sparse matrix $[A]$ and the $4m\times 1$ column vector $[C]$ are both known, so we invert the set of equations via Gaussian elimination to find the $4m\times 1$ column vector $[B]$. The scattered wave function at all points in space, namely, the a_l, b_l, c_l, d_l are obtained from the column vector $[B]$.

Bound levels in the inhomogeneous pairing potential are found from $\det[A(E_b)]=0$, where E_b is the bound-state energy. When any such bound levels exist, their wave functions must be normalized at each iteration so that

$$\int_{-\infty}^{\infty} [|u_b(x)|^2+|v_b(x)|^2]dx=1. \tag{A15}$$

The contribution each bound level makes to the total current is then found by applying the current operator, Eq. (4).

2. Scattering matrix method

To implement a scattering matrix method for the coefficients a,b,c,d in each region, we first reference the waves to a local origin in the region as

$$\begin{aligned} \psi_l(x)=\begin{bmatrix} u_l(x) \\ v_l(x) \end{bmatrix} &= \tilde{a}_l \begin{bmatrix} U_{al} e^{iq_l(x-x_l)} e^{i\tilde{\phi}_l/2} \\ V_{al} e^{-iq_l(x-x_l)} e^{-i\tilde{\phi}_l/2} \end{bmatrix} e^{ik_{al}(x-x_l)} \\ &+ \tilde{b}_l \begin{bmatrix} V_{bl} e^{iq_l(x-x_l)} e^{i\tilde{\phi}_l/2} \\ U_{bl} e^{-iq_l(x-x_l)} e^{-i\tilde{\phi}_l/2} \end{bmatrix} e^{ik_{bl}(x-x_l)} \\ &+ \tilde{c}_l \begin{bmatrix} V_{cl} e^{iq_l(x-x_l)} e^{i\tilde{\phi}_l/2} \\ U_{cl} e^{-iq_l(x-x_l)} e^{-i\tilde{\phi}_l/2} \end{bmatrix} e^{-ik_{cl}(x-x_l)} \\ &+ \tilde{d}_l \begin{bmatrix} U_{dl} e^{iq_l(x-x_l)} e^{i\tilde{\phi}_l/2} \\ V_{dl} e^{-iq_l(x-x_l)} e^{-i\tilde{\phi}_l/2} \end{bmatrix} e^{-ik_{dl}(x-x_l)}. \end{aligned} \tag{A16}$$

Equation (A16) implies a local-order parameter of the form

$$\Delta_l(x)=|\Delta_l|\exp i(2q_l[x-x_l]+\tilde{\phi}_l)=|\Delta_l(x)|e^{i\phi_l(x)}. \tag{A17}$$

We then solve a wave-matching problem for each type of injected particle, similar to the previous discussion, to obtain the scattering matrix[33,34] S_l from region l to $l+1$ as

$$\begin{bmatrix} \tilde{a}_{l+1} \\ \tilde{c}_{l+1} \\ \tilde{d}_l \\ \tilde{b}_l \end{bmatrix} = \begin{bmatrix} t_e & t_{Ae} & r'_e & r'_{Ae} \\ t_{Ah} & t_h & r'_{Ah} & r'_h \\ r_e & r_{Ae} & t'_e & t'_{Ae} \\ r_{Ah} & r_h & t'_{Ah} & t'_h \end{bmatrix} \begin{bmatrix} \tilde{a}_l \\ \tilde{c}_l \\ \tilde{d}_{l+1} \\ \tilde{b}_{l+1} \end{bmatrix}. \tag{A18}$$

For a superconducting segment having $m+1$ regions and m boundaries we obtain the overall scattering matrix $S_{1,m}$ entire structure by cascading the scattering matrices of each individual region

$$S_{1,m}=S_1\otimes S_2\otimes S_3\otimes\cdots\otimes S_m. \tag{A19}$$

The rules for cascading ($\otimes$) the scattering matrices are stated in Refs. 33 and 34. In this calculation we also retain the scattering matrices connecting the first region to all other regions, namely, $S_{1,2}, S_{1,3}, \ldots, S_{1,m}$.

The scattering matrix can also be used to find the quasiparticle wave functions everywhere throughout the device. Consider the scattering state produced by an electronlike wave incident on the conductor from the left. In the first region we then have

$$\begin{bmatrix} \tilde{a}_1 \\ \tilde{b}_1 \\ \tilde{c}_1 \\ \tilde{d}_1 \end{bmatrix} = \begin{bmatrix} 1 \\ [S_{1,m}]_{41} \\ 0 \\ [S_{1,m}]_{31} \end{bmatrix}. \tag{A20}$$

The waves in region 1 can then be used to find the waves in region $l+1$ by the scattering matrix equation

$$\begin{bmatrix} \tilde{a}_{l+1} \\ \tilde{c}_{l+1} \\ \tilde{d}_1 \\ \tilde{b}_1 \end{bmatrix} = S_{1,l} \begin{bmatrix} \tilde{a}_1 \\ \tilde{c}_1 \\ \tilde{d}_{l+1} \\ \tilde{b}_{l+1} \end{bmatrix}. \tag{A21}$$

Resonant quasiparticle energy levels are defined by the poles of the scattering matrix. The resonance energy E_b is determined by

$$\frac{1}{[S_{1,m}(E=E_b)]_{ij}}=0, \tag{A22}$$

where the subscript ij denotes any element of the scattering matrix. For a ballistic junction, there are generally two such sets of poles, one for right-moving electrons and another for left-moving electrons. The bound-states wave function so determined must be normalized according to Eq. (A15) during each iteration.

3. Updating the pair potential

After the nth iteration, where the order parameter from Eq. (A1) can be written

$$\Delta_n(x)=|\Delta_n(x)|e^{i\phi_n(x)}, \tag{A23}$$

we determine the the supercurrent flow q_l^{n+1} in the lth region for the $(n+1)$st iteration by

$$2q_l^{n+1}=\frac{\phi_n(x_l)-\phi_n(x_{l-1})}{x_l-x_{l-1}}, \tag{A24}$$

and the phase angle ϕ_l^{n+1} from

$$2q_l^{n+1}\left(\frac{x_l+x_{l-1}}{2}\right)+\phi_l^{n+1}=\phi_n([x_l+x_{l-1}]/2). \tag{A25}$$

APPENDIX B: CURRENT CARRIED BY ANDREEV LEVELS

In this appendix we give an analytic proof that the bound Andreev energy levels carry no net current (at zero temperature) in a perfectly ballistic, uniform-width, SNS junction. We also prove that the continuum current is equal to the total current in such a junction. This energy distribution of the electrical current in a uniform-width SNS junction is in contrast to the SNS point contact, where the bound Andreev levels carry all the supercurrent and the continuum levels carry no current.

The current carried by bound Andreev levels in a ballistic SNS junction without a superfluid flow $(q=0)$ is given by[6]

$$I_n^{\pm}=\pm\frac{ev_F}{L+2\xi(E_n(q=0))}. \tag{B1}$$

Here the decay length is

$$\xi(E)=\xi_0\frac{\Delta}{\sqrt{\Delta^2-E^2}}. \tag{B2}$$

The superscript $\pm$ in Eq. (B1) refers to the right-moving $(+)$ and left-moving $(-)$ electronlike quasiparticle levels.[6]

Equation (B1) for the electrical current does not hold as written when the SNS junction is subject to a superfluid flow. This is because the appropriate decay length is determined by the separation of the Andreev level from the nearest band edge, rather than from $E=0$. We therefore introduce the energy separation $\epsilon\geqslant 0$ of the Andreev level from the band edge as shown in Fig. 13(a). We then find the appropriate coherence distance in terms of ϵ as

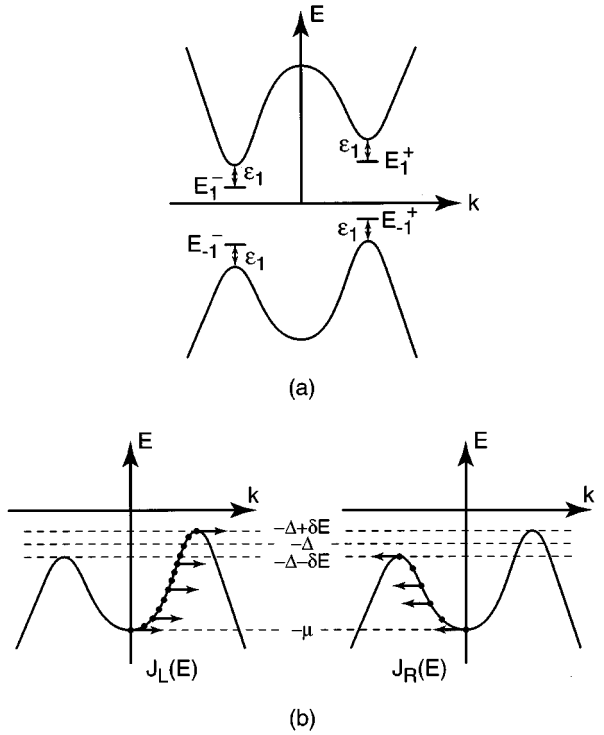

FIG. 13. (a) Bound-energy levels subject to a superfluid flow. (b) Current-carrying states in the continuum subject to a superfluid flow.

$$\xi(\epsilon)=\xi_0\frac{\Delta}{\sqrt{2\Delta\epsilon-\epsilon^2}}. \tag{B3}$$

The corresponding electrical current carried by each Andreev level when $q\neq 0$ can then be written as

$$I_n^{\pm}=\pm\frac{ev_F}{L+2\xi(\epsilon_n^{\pm})}. \tag{B4}$$

Equations (B3) and (B4) remain valid under a superfluid flow.

We show the energy-level spectrum of an SNS junction with a single energy level subject to a superfluid flow schematically in Fig. 13(a). Note the labeling scheme we employ in this appendix has energies E_n with $n>0$ above the Fermi level and $n<0$ below the Fermi level. There is no $n=0$ energy level. Because the superconducting energy bands near the gap edge shift essentially rigidly with the superfluid flow, the separation of the Andreev levels from the gap edge will obey the relation

$$\epsilon_n^+=\epsilon_{-n}^+=\epsilon_n^-=\epsilon_{-n}^-. \tag{B5}$$

Equation (B5) is also shown schematically in Fig. 13(a).

We now sum the bound-level currents to obtain the total discrete current I_D as

$$I_D=\sum_{n,\alpha} I_n^{\alpha}f(E_n^{\alpha}). \tag{B6}$$

The index $\alpha=\pm$ in Eq. (B6), again denoting the left- and right-moving electronlike quasiparticle states. By reference

to the symmetry of the energy levels in Eq. (B5), we can infer from Eqs. (B3) and (B4) that

$$I_n^+ = I_{-n}^+ = -I_n^- = -I_{-n}^-, \tag{B7}$$

together with

$$f(E_{-n}^+) + f(E_n^-) = 1 \tag{B8}$$

and

$$f(E_{-n}^-) + f(E_n^+) = 1. \tag{B9}$$

Equations (B6)–(B9) give

$$I_D = 2\sum_{n>0} I_n^+ [f(E_n^+) - f(E_n^-)]. \tag{B10}$$

Equation (B10) shows that the discrete levels carry zero current at zero temperature [when $f(E_n^+) = f(E_n^-)$] or when the superfluid flow is zero [$E_n^+ = E_n^-$]. The reason the discrete level currents sum to zero is because the current carried by each level is approximately the same under a superfluid flow as at zero flow, namely, $I_n^{\pm}(q) \simeq I_n^{\pm}(q=0)$. If the Andreev levels nearly rigidly follow the band edge under a superfluid flow, that is, $\epsilon_n^{\pm}(q) \simeq \epsilon_n^{\pm}(q=0)$, then both the decay length and electrical current appropriate for each Andreev level remain unchanged when the SNS junction is subject to a superfluid flow.

If the bound Andreev levels carry zero net current at zero temperature, then the continuum levels in the SNS junction must carry the total current. We prove this with reference to Fig. 13(b), showing the electronlike quasiparticle states injected from either superconductor. The current I_C from the continuum energy levels having $E<0$ can be written as

$$I_C = \int_{-\mu}^{-\Delta+\delta E} J_R(E) f(E) dE - \int_{-\mu}^{-\Delta-\delta E} J_L(E) f(E) dE, \tag{B11}$$

where $\delta E = m v_F (\hbar q/m)$. We make a change of integration variable to rewrite Eq. (B11) as

$$I_C = \int_{-\mu-\delta E}^{-\Delta} J_R(E' + \delta E) f(E' + \delta E) dE' - \int_{-\mu+\delta E}^{-\Delta} J_L(E'' - \delta E) f(E'' - \delta E) dE. \tag{B12}$$

We simplify Eq. (B12) to the case of zero temperature, where $f(E)=1$ for $E<0$. Furthermore, we have $J_R(E' + \delta E) = J_L(E'' - \delta E)$ near the superconducting gap edges, since both are simply the same function shifted in energy by the superfluid flow. The only net contribution to Eq. (B12) therefore comes near the band bottom, where we have

$$I_C \simeq J_R(-\mu) 2\delta E. \tag{B13}$$

Ballistic transport far from the band edge means the current density is $J_R(-\mu) \simeq e/h$, leaving $I_C \simeq (e/h)(2 m v_F v_s)$. Using the critical velocity of the bulk superconductor $v_d = \Delta/p_F$, we can rewrite the continuum current at zero temperature as $I_c = (e/h)(2\Delta)(v_s/v_d)$. The hole contribution doubles the current contributed by the injected electrons, leaving

$$I_C \simeq \left(\frac{4e\Delta}{h}\right)\left(\frac{v_s}{v_d}\right). \tag{B14}$$

The continuum current from Eq. (B14) is equal to the total current in the uniform-width, ballistic SNS junction at zero temperature.

[1] C.W.J. Beenakker and H. van Houten, Phys. Rev. Lett. **66**, 3056 (1991).

[2] See the collection of articles in *Proceedings of the NATO Advanced Research Workshop on Mesoscopic Superconductivity*, edited by F.W.J Hekking, G. Schon, and D.V. Averin [Physica B **203**, 201 (1994)].

[3] B.J. van Wees, K.M.H. Lenssen, and C.J.P.M. Harmans, Phys. Rev. B **44**, 470 (1991).

[4] C.W.J. Beenakker, Phys. Rev. Lett. **67**, 3836 (1991).

[5] A. Furusaki, H. Takayanagi, and M. Tsukada, Phys. Rev. Lett. **67**, 132 (1991); Phys. Rev. B **45**, 10 563 (1992).

[6] P.F. Bagwell, Phys. Rev. B **46**, 12 573 (1992).

[7] G.E. Rittenhouse and J.M. Graybeal, Phys. Rev. B **49**, 1182 (1994).

[8] U. Gunsenheumer, U. Schüssler, and R. Kümmel, Phys. Rev. B **49**, 6111 (1994).

[9] M. Hurd and G. Wendin, Phys. Rev. B **49**, 15 258 (1994).

[10] L. Chang and P.F. Bagwell, Phys. Rev. B **49**, 15 853 (1994).

[11] A. Martin-Rodero, F.J. Garcia-Vidal, and A. Levy Yeyati, Phys. Rev. Lett. **72**, 554 (1994); A. Levy Yeyati, A. Martin-Rodero, and F.J. Garcia-Vidal, Phys. Rev. B **51**, 3743 (1995).

[12] J. Sánchez Cañizares and F. Sols, J. Phys. Condens. Matter **7**, L317 (1995).

[13] A. Martin and C.J. Lambert, Phys. Rev. B **51**, 17 999 (1995).

[14] P.F. Bagwell, Phys. Rev. B **49**, 6841 (1994).

[15] R. Kümmel, Z. Phys. **218**, 472 (1969).

[16] W.N. Mathews, Jr., Physica Status Solidi B **90**, 327 (1978).

[17] F. Sols and J. Ferrer, Phys. Rev. B **49**, 15 913 (1994).

[18] A. Furusaki and M. Tsukada, Solid State Commun. **78**, 299 (1991).

[19] J. Bardeen and J.L. Johnson, Phys. Rev. B **5**, 72 (1972).

[20] H. Plehn, U. Gunsenheimer, and R. Kümmel, J. Low Temp. Phys. **83**, 71 (1991).

[21] A.F. Andreev, Zh. Éksp. Teor. Fiz. **46**, 1823 (1964) [Sov. Phys. JETP **19**, 1228 (1964)]; **49**, 655 (1966) [**22**, 455 (1966)].

[22] I.O. Kulik, Zh. Éksp. Teor. Fiz. **57**, 1745 (1969) [Sov. Phys. JETP **30**, 944 (1970)].

[23] R. Landauer, J. Phys. Condensed Matter **1**, 8099 (1989).

[24] B.P. Stojković and O.T. Valls, Phys. Rev. B **51**, 3186 (1995).

[25] P.G. de Gennes, *Superconductivity of Metals and Alloys* (Benjamin, New York, 1966).

[26] S. Datta, P.F. Bagwell, and M.P. Anantram, Phys. Low Dimen. Struct. **3**, 1 (1996).

[27] Y. Tanaka and M. Tsukada, Phys. Rev. B **47**, 287 (1993),

[28] G.E. Blonder, M. Tinkham, and T.M. Klapwijk, Phys. Rev. B **25**, 4515 (1982).

[29] L. Chang, S. Chaudhuri, and P.F. Bagwell, Phys. Rev. B **54**, 9399 (1996).

[30] V. Ambegaokar and A. Baratoff, Phys. Rev. Lett. **10**, 486 (1963); **11**, 104 (1963).

[31] A.A. Abrikosov, L.P. Gorkov, and I.E. Dzyaloshinski, *Methods of Quantum Field Theory in Statistical Physics* (Prentice-Hall, Englewood Cliffs, NJ, 1963). See Eqs. (32.3)–(32.6).

[32] *CRC Standard Mathematical Tables*, 26th ed. (CRC, Boca Raton, FL, 1981), p. 12.

[33] M. Cahay, M. McLennan, and S. Datta, Phys. Rev. B **37**, 10 125 (1988).

[34] R.A. Riedel and P.F. Bagwell, Phys. Rev. B **48**, 15 198 (1993).